Int. J. Electrochem. Sci., 11 **(2016)** 6959 – 6975, doi: 10.20964/2016.08.48

International Journal of ELECTROCHEMICAL SCIENCE
www.electrochemsci.org

Aqueous Extract of *Salvadora Persica* as a Novel Green Corrosion Inhibitor for Low-Alloy Steel in Acidic Media - *Part I*

Aliaa A. M. Hassan[1], *Hesham T.M. Abdel-Fatah*[2,*]

[1] Faculty of Science and Arts in Al-Ardha, Jazan University, Al-Ardha, Jazan, Saudi Arabia.
[2] Department of Corrosion Research, Central Chemical Laboratories, EEHC, Cairo, EGYPT
[*]E-mail: hesham_tm@yahoo.com

Received: 13 April 2016 / *Accepted:* 7 June 2016 / *Published:* 7 July 2016

The corrosion inhibition characteristics of aqueous extract of *Salvadora Persica* (AESP) on low chromium-molybdenum steel (ASTM A213) grade T2 (0.5Cr- 0.5Mo) in 1M hydrochloric acid solutions has been studied chemically and electrochemically at different temperatures. The protection efficiency in absence and presence of AESP was investigated by using mass loss method, Inductively Coupled Plasma Optical Emission Spectrophotometer (ICP-OES), as will as potentiodynamic polarization, electrochemical impedance spectroscopy (EIS), and electrochemical frequency modulation (EFM) techniques. The protection efficiency was found to increase with a corresponding increase in the AESP concentration and decrease with temperature. Amongst the different adsorption isotherms, the studied compound more closely followed the Temkin isotherm. The values of standard free energy of adsorption (ΔG^{o}_{ads}) revealed that AESP is adsorbed on the low-alloy steel surface via physisorption mechanism.

Keywords: acid cleaning, hydrochloric acid, low-alloy steel, corrosion inhibition, Salvadora persica, mass loss, EIS, EFM, ICP-OES.

1. INTRODUCTION

Low-alloy steels are widely employed in the power and petrochemical industries for boilers piping, and chemical reaction vessels. ASTM A213 grade T2 (0.5Cr- 0.5Mo) steels are used as tubes for heat exchangers, plates and forgings for pressure vessels. The corrosion resistance are improved by addition of 0.5% of chromium and the creep strength of this steel is improved by addition of 0.5% of molybdenum [1,2].

In the industrial processes the usage of acid solutions is phenomenal and is used extensively for cleaning, descaling, and oil well acidizing. The acid solutions (e.g. hydrochloric, sulphuric, sulfamic,

citric acids) works well to remove the waterside unwanted scales, rusts and deposits on the metal surface [3,4]. In order to protect metal corrosion in acidic media the inhibitors are used, they are highly effective and economic [5,6].

Even in today's time the using of corrosion inhibitor compounds are harmful to the humans and to the environment. Therefore, the need of hour is to use environmental friendly inhibitors for safer and healthy life. In recent times, several studies were carried out on the inhibition of corrosion of metals by plants extract. The plant extracts, in addition to being environmentally friendly, they are low-cost, easily available and renewable [7–13].

Arak tree (*Salvadora Persica*) is traditionally used for the treatment of oral infections. Also, their young roots, stems and branches are used as toothbrush [14-16]. *Salvadora Persica* has different names in different societies. For instance, miswak, siwak, or arak.

Pharmacological studies have shown that it has a number of proven medicinal applications. Its leaves, root, bark, fruit and seed, all have some medicinal benefits [15-19]. On the other hand, the chemical constituents of Salvadora Persica had been reported earlier [20-25].

It is worth mentioning here that the published research related to the corrosion inhibitive properties of *Salvadora Persica* are almost rare [26]. Therefore, the present study aims to fill this gap and investigate the inhibitive properties of aqueous extract of Salvadora Persica (AESP) on the corrosion behaviour of low-alloy steel T2 in 1 M hydrochloric acid solution. Moreover, this article is a continuation of a series of publications dedicated to exploration of eco-friendly corrosion inhibitors [27-30].

2. EXPERIMENTAL

2.1. Inhibitor preparation

The arak tree (*Salvadora persica*) was collected from Jazan, Saudi Arabia. 10 grams of dried leaves, roots and fruits of arak tree were cut into small pieces and were soaked in ultra-pure water (500 ml) and refluxed for 5 h. The refluxed solution was filtered to remove any contamination and then was concentrated to 100 ml. The concentrated solution was used to prepare solutions of different concentrations by dilution method in order to study the corrosion inhibition characteristics of Salvadora persica.

One Molar of hydrochloric acid was prepared by dilution of analytical grade HCl (37%) with ultra-pure water. All experiments were carried out in open air and unstirred solutions.

2.2. Material preparation

The specimens used for corrosion tests were low-alloy steel ASTM A213 grade T2 coupons having the following composition (wt %): 0.31 Si, 0.47 Mn, 0.57 Cr, 0.48 Mo and the rest being Fe (98.37 %). Prior to all measurements, the steel electrodes were mechanically abraded with emery

papers from 600 to 1200 grades, degreased with acetone in an ultrasonic bath, then rinsed with ultra-pure water and finally dried by warm air before use.

2.3. Mass loss method

The measurements of changes in the mass were performed on rectangular coupons of size 1.5 cm x 1 cm x 0.2 cm with total exposed area of (4 cm^2). The loss of mass was determined by weighing the cleaned samples before and after 24 hours immersion in the tested solutions at different temperatures.

2.4. Inductively coupled plasma optical emission spectroscopy (ICP-OES) method

Quantitative analysis of the major metal iron (Fe) content present in the corrosive solutions has been performed by using Perkin Elmer Model Optima 8300 Inductively Coupled Plasma Optical Emission Spectrometry (ICP-OES).

At its core the ICP sustains a temperature of approximately 10000 K, so the aerosol is quickly vaporized. Analyte elements are liberated as free atoms in the gaseous state. Sufficient energy is often available to convert the atoms to ions and subsequently promote the ions to excited states. Both the atomic and ionic excited state species may then relax to the ground state via the emission of a photon. Thus the wavelength of the photons can be used to identify the element type, and the content of each element is determined based on the photon rays' intensity.

2.5. Electrochemical studies

Electrochemical measurements were conducted in a conventional three-electrode cell of capacity 150 ml, consisting of a steel electrode embedded in epoxy resin so that the cross sectional area 1 cm^2 is only exposed to the solution, as working electrode, while a saturated calomel electrode (SCE) and a platinum electrode were used as reference and counter electrode, respectively.

The electrode was held in the test solution for 30 minutes which provided sufficient time for E_{corr} to attain a reliable stable state in the open circuit potential (E_{ocp}).

The anodic and cathodic potentiodynamic polarization measurements were performed in 1 M HCl solution, containing different concentrations of the tested inhibitor, by changing the electrode potential automatically from -1000 to +50 mV versus corrosion potential at a scan rate 1 mVs^{-1}.

Electrochemical impedance spectroscopy (EIS) measurements were made at corrosion potential (E_{corr}) over the frequency range from 100,000 to 1 Hz at an amplitude of 10 mV and scan rate of 10 points per decade.

Electrochemical frequency modulation (EFM) is a recent technique provides a new tool for electrochemical corrosion monitoring in which two sinusoidal potential signals are summed and applied to a corrosion sample through a potentiostat. The resulted current is measured and the time-domain data is converted to the frequency domain. This frequency domain is used to measure the

signal at the applied fundamental frequencies, at harmonics of the fundamental frequencies, and at intermodulation frequencies. By the appropriate mathematical manipulation, the large peaks are used to directly determine the values of corrosion current density (I_{corr}), corrosion rate, Tafel constants (β_c and β_a) and the causality factors (CF2 & CF3).

The features and theory of EFM technique were reported previously [31]. The EFM measurements are performed with applying potential perturbation signal with amplitude of 10 mV with two sine waves of 2 and 5 Hz and the base frequency was 1 Hz, so the waveform repeats after 1 s.

All Electrochemical experiments were carried out using Gamry PCI300/4 Potentiostat/Galvanostat/Zra analyzer, DC105 corrosion software, EIS300 electrochemical impedance spectroscopy software, EFM140 electrochemical frequency modulation software and Echem Analyst 5.21 for results plotting, graphing, data fitting & calculating.

3. RESULTS AND DISCUSSION

3.1. Mass loss results:

The corrosion of low-alloy steel (LAS) in static 1 M hydrochloric acid solutions in the absence and the presence of 500 ppm of AESP were studied at different temperatures with an exposure time of 24 hours using mass loss technique.

The corrosion rate in units of millimeters per year (mm/year) can be represented by the following equation [32]:

$$\text{Corrosion rate (mm/year)} = 3.16 \text{ x } \left(\frac{W}{DAt} \right) \qquad (1)$$

where W is the mass loss in milligrams, D is the density in g/cm^3 (D = 7.88), A is the area in square inches (A = 0.62) and t is the time of exposure in hours (t = 24).

Table 1 shows the calculated mass loss (mg) and corrosion rate (mm/year) for LAS in 1 M hydrochloric acid solutions in the absence and presence of AESP at different temperatures.

Table 1. Mass loss results of LAS in 1 M HCl solution in the absence and presence of 500 ppm of AESP at different temperatures

Temp (K)	Concentration of inhibitor (ppm)	Mass Loss (mg)	Corrosion Rate (mm/year)	PE %
303	0	329.3	38.19	0.00
	500	18.6	2.16	94.35
313	0	543.7	63.06	0.00
	500	59.3	6.88	89.09
323	0	787.6	63.06	0.00
	500	95.6	11.09	82.42
333	0	1014.6	91.35	0.00
	500	198.5	23.02	74.80

The protection efficiency (PE %) of AESP was calculated under different experimental conditions by using the following equation:

$$PE\% = \frac{CR^o - CR}{CR^o} \times 100 \qquad (2)$$

where CR^o and CR are the corrosion rate obtained from mass loss measurements in the absence and presence of inhibitor, respectively. The calculated values of protection efficiency (PE %) were also listed in Table 1.

The protection efficiency (PE %) increases in presence of AESP as a result of increasing surface coverage by inhibitor species. However, at a given inhibitor concentration, the PE % of AESP decreases with rising the temperature. This behaviour is due to the decrease in the strength of adsorption process by increasing temperature, suggesting that physical adsorption may be the type of adsorption of the inhibitor on the sample surfaces [33].

3.2. Inductively Coupled Plasma Optical emission spectroscopy results:

The iron ion content in the corrosive solutions in the absence and the presence of 500 ppm of AESP were identified at different temperatures with an exposure time of 24 hours to test the effect of AESP on the corrosion process using ICP-OES technique.

Inspection of obtained results, given in Table 2, clearly shows that the reduction of iron ions concentrations when AESP was presented in the corrosive solution. These results are a further evidence of the inhibiting effect of AESP against corrosion of low-alloy steel.

Table 2. ICP-OES results of LAS in 1 M HCl solution in the absence and presence of 500 ppm of AESP at different temperatures

Temp (K)	Concentration of inhibitor (ppm)	Fe Concentration (mg/L)	PE %
303	0	2449.56	0.00
	500	111.87	95.43
313	0	4997.61	0.00
	500	496.89	90.06
323	0	7817.93	0.00
	500	1504.28	80.76
333	0	11234.76	0.00
	500	2987.12	73.41

The protection efficiency (PE %) of AESP was calculated under different experimental conditions by using the following equation:

$$PE\% = \frac{Fe^o - Fe}{Fe^o} \times 100 \qquad (3)$$

where Fe^{o} and Fe are the concentration of iron obtained from ICP-OES measurements in the uninhibited and inhibited solutions, respectively. The calculated values of protection efficiency (PE %) were summarised in Table 2.

3.3. Potentiodynamic polarization results:

The effect of an increased concentration of aqueous extract of Salvadora Persica (AESP) on the anodic and cathodic polarization curves of low-alloy steel (LAS) in 1 M HCl solution at 303 K is represented in Figure 1 as an example. Inspection of Figure 1 indicates that after the addition of AESP into 1 M HCl solution, both anodic and cathodic reactions of the mild steel corrosion are retarded.

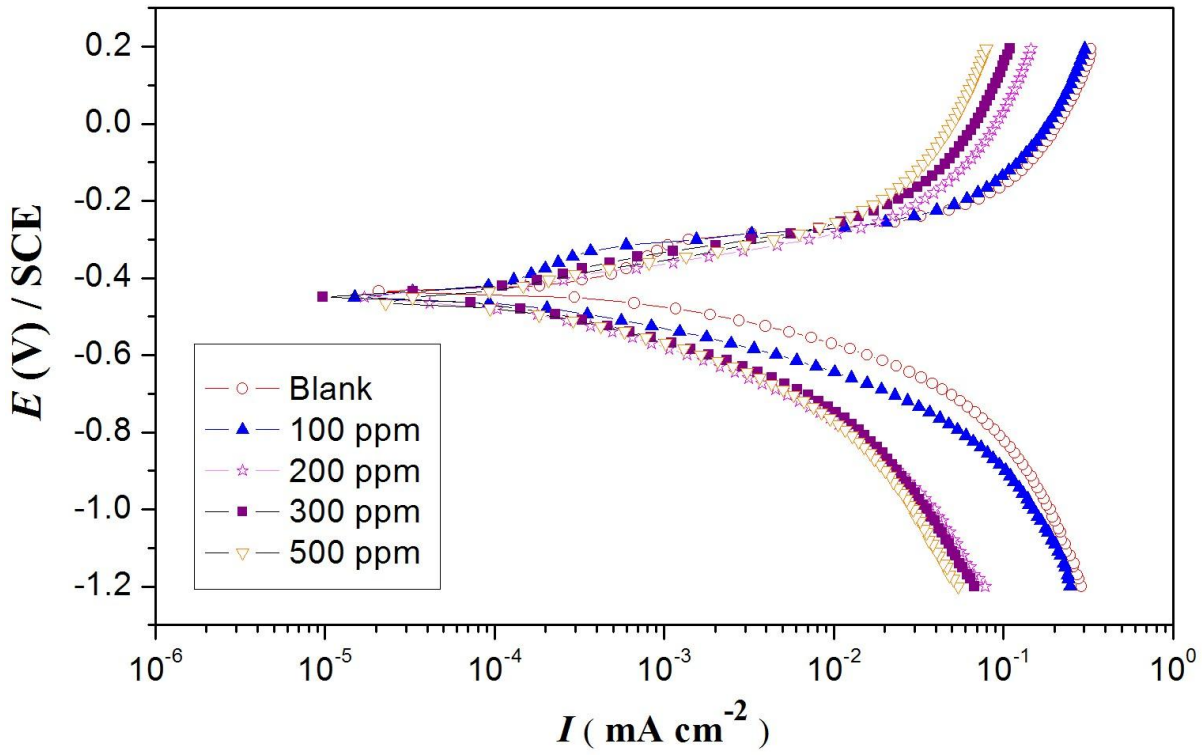

Figure 1. Tafel plots of LAS in 1 M HCl solution in the absence and presence of different concentrations of AESP at 303 K.

The potentiodynamic polarization parameters including corrosion current densities (I_{corr}), corrosion potential (E_{corr}), cathodic Tafel slope (β_c), and anodic Tafel slope (β_a) of mild steel in 1.0 N HCl containing various concentrations of AESP at different temperatures were presented in Table 3.

Inspection of Table 3 reveals that I_{corr} decreases gradually with the increasing concentrations of AESP, indicating that the inhibitor has an effective inhibition for the corrosion of LAS in HCl acid solution. The presence of AESP in HCl solution resulting in a slight shift of corrosion potential (E_{corr}) toward the negative direction in comparison with the inhibitor free solution, reveals that the compound

acts as a mixed-type inhibitor [34,35]. Moreover, the addition of AESP, causes slight change of both β_c and β_a , indicating that the corrosion mechanism of LAS does not change [36].

Table 3. potentiodynamic polarization results of LAS in 1 M HCl solution with various concentrations of AESP at different temperatures

Temp. (K)	Concentration of inhibitor (ppm)	E_{corr} (mV)	β_a (mV dec^{-1})	β_c (mV dec^{-1})	I_{corr} (μA cm^{-2})	PE %
303	0	-483	74.36	203.61	1211	0.00
	100	-479	73.75	201.36	724.4	40.18
	200	-481	71.95	198.35	514.8	57.49
	300	-478	72.56	200.12	244.6	79.80
	500	-485	73.15	201.94	68.28	94.36
313	0	-490	71.46	201.18	1616	0.00
	100	-488	70.81	199.68	1147	29.02
	200	-489	71.70	201.47	664.8	58.86
	300	-486	72.56	199.58	453.1	71.96
	500	-485	69.62	198.35	179.6	88.89
323	0	-479	74.25	200.33	2527	0.00
	100	-482	72.48	200.18	1706	32.49
	200	-483	70.28	199.87	1293	48.83
	300	-487	71.59	198.55	874.5	65.39
	500	-485	71.08	200.01	509.3	79.85
333	0	-487	72.19	202.14	3091	0.00
	100	-483	70.78	201.66	2444	20.93
	200	-479	71.22	202.17	1947	37.01
	300	-486	72.18	200.51	1377	55.45
	500	-478	72.84	201.90	789.6	74.45

The protection efficiency (PE %) of AESP was calculated by the use of the following equation:

$$PE\% = \frac{I^{o}_{corr} - I_{corr}}{I^{o}_{corr}} \times 100 \qquad (4)$$

where I^{o}_{corr} and I_{corr} represent corrosion current density values without and with inhibitor, respectively.

The PE % values of different AESP concentrations and at different temperatures are included in Table 3. At a given temperature, the PE % increases with the increasing AESP concentration as a result of increasing adsorption and surface coverage on the steel surface. Therefore, the inhibition behavior is appeared through the reduction of the reaction area on the surface of the corroding metal [37]. However, at a certain concentration of AESP, the PE % decreases with increasing of solution temperature.

3.4. Electrochemical impedance spectroscopy (EIS) results

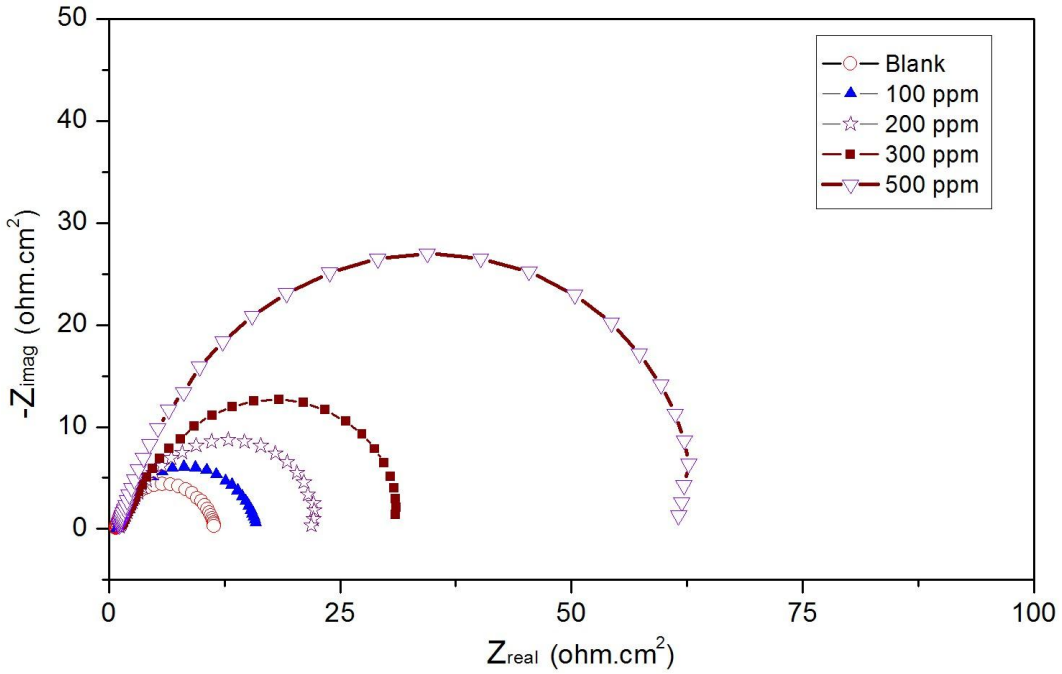

Figure 2. Nyquist diagrams of LAS in 1 M HCl solution in the absence and presence of different concentrations of AESP at 323 K.

Figure 2 illustrates the Nyquist diagrams for LAS in 1 M HCl solutions in both the absence and presence of four different concentrations of AESP at 323 K as an example. The impedance spectra exhibit one single capacitive loop, which indicates that the corrosion of steel is mainly controlled by a charge transfer process [38].

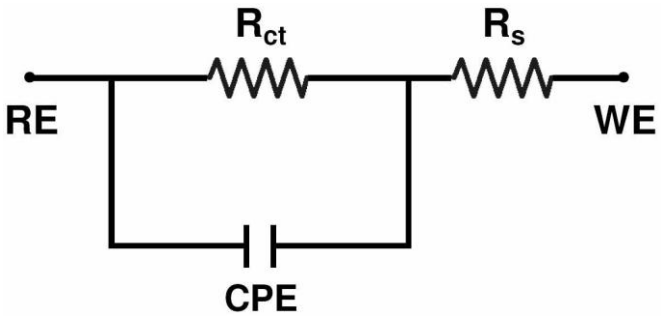

Figure 3. Electrical equivalent circuit representing the fitting of EIS data

It is obvious that the Nyquist diagrams in Figure 2 are not perfect semicircles. The depressed form of semicircles has been attributed to the frequency dispersion as a result of the heterogeneity or roughness of electrode surface [39]. The EIS results are simulated by the equivalent circuit shown in Figure 3. The constant phase element (*CPE*) was introduced in the circuit instead of a pure double layer capacitor to give a more accurate fit [40]. In this circuit, R_s is the solution resistance, R_{ct} presents

the charge transfer resistance, and *CPE* represents the constant phase elements used to replace the double layer capacitance (C_{dl}). The fitted impedance parameters of LAS in 1 M HCl in absence and presence of various concentrations of AESP at different temperatures were listed in Table 4.

According to the data in Table 4, the values of charge transfer resistance (R_{ct}) increase, while the double layer capacitance (C_{dl}) decreases as the concentration of ARESP is increased from 100 ppm to 500 ppm. This is due to the increase in the surface coverage by the inhibitor molecules leading to an increase in the thickness of the electrical double layer which is responsible for the decrease in C_{dl} values. This suggests that AESP acts by adsorption at the metal/solution interface by the gradual replacement of water molecules and the resulted adsorption film isolates the metal surface from the corrosive medium and decreases metal dissolution. The conclusions above can be explained on the basis that the electrostatic adsorption of the inhibitor species at the metal surface leads to the formation of a physical protective film that retards the charge transfer process and therefore inhibits the corrosion reactions and so increases the value of (R_{ct}). Moreover, the adsorbed inhibitor species decrease the electrical capacity of the electrical double layer at the electrode/solution interface and therefore decrease the values of (C_{dl}) [41,42].

Table 4. EIS results of LAS in 1 M HCl solution with various concentrations of AESP at different temperatures

Temp. (K)	Concentration of inhibitor (ppm)	C_{dl} (μF cm^{-2})	R_{ct} (ohm cm^2)	PE %
303	0	931.6	20.37	0.00
	100	568.3	32.98	38.24
	200	410.3	46.41	56.11
	300	200.1	97.15	79.03
	500	47.3	414.60	95.09
313	0	1402.0	13.42	0.00
	100	947.4	19.92	32.63
	200	650.2	32.14	58.25
	300	405.8	49.77	73.04
	500	144.3	127.54	89.48
323	0	1912.0	10.18	0.00
	100	1388.0	14.01	27.34
	200	995.7	19.71	48.35
	300	669.5	28.72	64.55
	500	319.6	49.21	79.31
333	0	2700.0	7.23	0.00
	100	2110.0	9.27	22.01
	200	1640.0	11.98	39.65
	300	1182.0	16.67	56.63
	500	647.0	31.34	76.93

Because the reciprocal of charge transfer resistance ($1/R_{ct}$) is directly proportional to the rate of corrosion, the protection efficiency (PE %) was calculated by comparing the values of the charge transfer resistance in the absence (R^{o}_{ct}) and presence (R_{ct}) of inhibitor using the following relationship:

$$\text{PE \%} = \frac{R_{ct} - R^{o}_{ct}}{R_{ct}} \times 100 \qquad (5)$$

The values of PE % of AESP at different temperatures were listed in Table 4. Through Table 4 it is evident that the protection efficiency of AESP depends on both the concentration of the inhibitor and temperature. PE % of AESP increases with increasing inhibitor concentration and decreases with increasing temperature, which indicates the weakness of adsorption of AESP on the steel surface.

3.5. Electrochemical frequency modulation (EFM) results:

Figure 4 - as an example - shows the typical EFM plots for LAS in 1 M HCl in both the absence and presence of 500 ppm of AESP at 313 K.

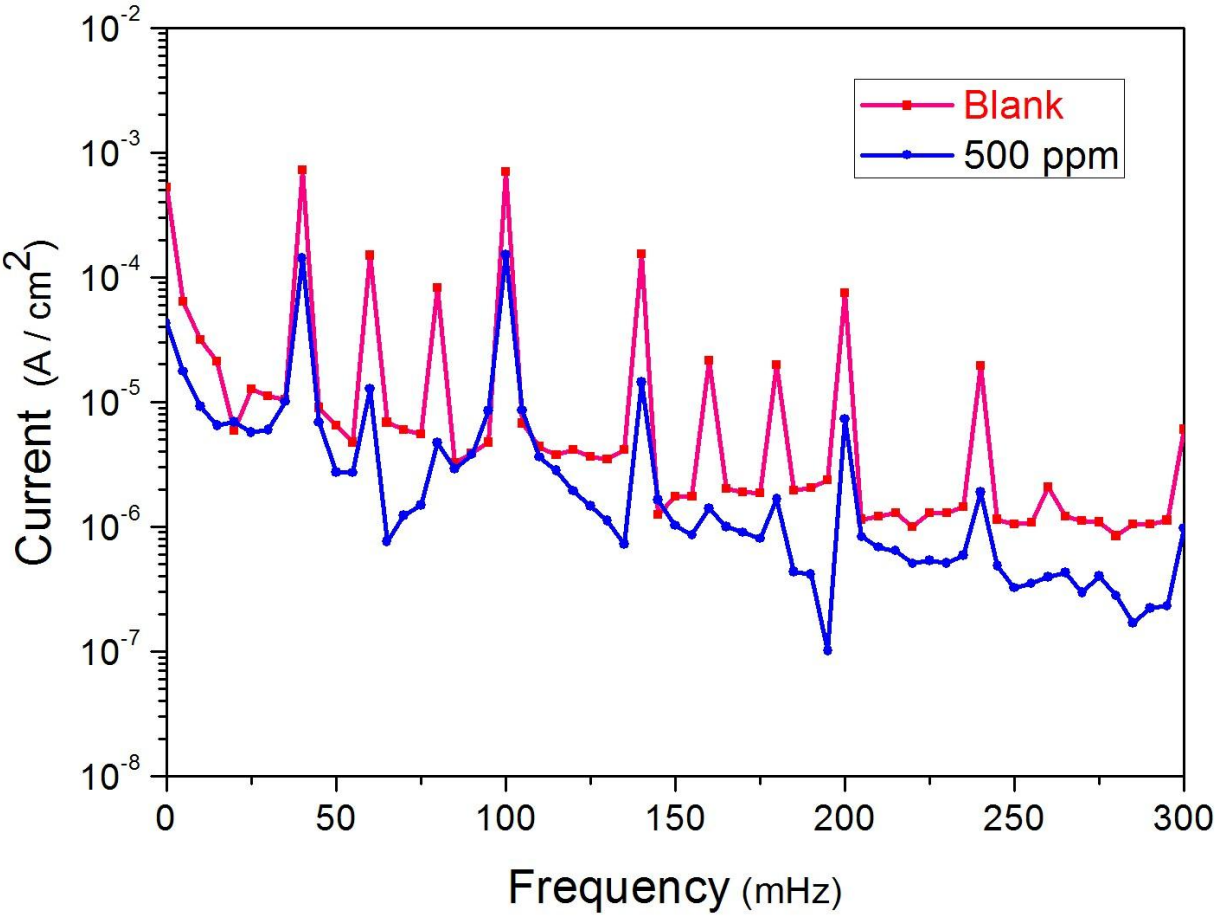

Figure 4. Intermodulation Spectra of LASS in 1 M HCl solution in the absence and presence of 500 ppm of AESP at 313 K.

The corrosion kinetic parameters obtained from the EFM technique, including corrosion current density (I_{corr}), Tafel constants (β_c and β_a) and the causality factors (CF2 and CF3) are given in Table 5.

The protection efficiency (PE %) of AESP was calculated from the corrosion current density by using the same Equation 1, and provided in Table 5.

Table 5. EFM results of LAS in 1 M HCl solution with various concentrations of AESP at different temperatures

Temp. (K)	Concentration of inhibitor (ppm)	β_a (mV dec^{-1})	β_c (mV dec^{-1})	CF2	CF3	I_{corr} (μA cm^{-2})	PE %
303	0	82.7	172.8	1.99	2.87	1154.0	0.00
	100	80.2	171.1	2.125	3.181	691.2	40.10
	200	81.5	170.6	1.79	2.99	500.4	56.64
	300	83.2	178.4	1.98	2.76	240.0	79.20
	500	83.1	179.1	2.00	2.85	70.14	93.92
313	0	60.5	188.3	1.909	3.001	1589.0	0.00
	100	58.2	186.4	1.787	3.196	1120.0	29.52
	200	59.7	189.7	2.087	2.841	701.4	55.86
	300	61.4	190.0	1.917	3.216	481.7	69.69
	500	61.8	188.8	2.311	3.071	207.6	86.94
323	0	63	187	1.832	3.124	2502	0.00
	100	60	188	1.927	2.621	1802	27.98
	200	58.7	189.2	2.289	3.221	1401.0	44.00
	300	60.3	188.9	2.104	2.946	924.3	63.06
	500	61.3	187.7	1.870	2.705	519.6	79.23
333	0	59.0	189.7	2.381	2.886	3078	0.00
	100	60.73	185.76	2.00	2.74	2517	18.23
	200	61.1	187.3	1.928	3.247	2002	34.96
	300	58.9	186.6	1.812	3.258	1366.0	55.62
	500	62.4	189.9	2.214	2.911	750.0	75.63

It can be seen from Table 5 that the values of corrosion current density (I_{corr}) of MS decrease and the protection efficiency (PE %) increases with the increasing inhibitor concentration. The increase in effectiveness of inhibition with increasing inhibitor concentration indicates that more inhibitor molecules are adsorbed on the metal surface providing wider surface coverage and AESP acts as an adsorption inhibitor [43]. The values of β_c and β_a do not show any appreciable change indicating that the studied inhibitor is a mixed-type inhibitor [44]. Moreover, the causality factors CF2 and CF3 are very close to the theoretical values 2.0 and 3.0, respectively, indicating that the measured data are reliable [31].

It is worth mentioning that the results obtained from the electrochemical techniques are in good agreement and also follow almost the same trends.

3.6. Adsorption isotherm

The study was done on the nature of adsorption of the inhibitor molecules on the steel surface in order to derivate the appropriate isotherm of adsorption. In general, there are two main types of

adsorption: physical adsorption and chemisorption, which are affected by the nature as well as the charge of the metal, the chemical structure of the inhibitor, and the type of electrolyte.

In the present work, Temkin adsorption isotherm is the appropriate one to fit the experimental results obtained from different methods, which can be described by plotting of the degree of surface coverage ($\theta = EI\ \% / 100$) versus the logarithm of inhibitor concentration (C_{inh}), which yields straight lines [45,46]. Figure 5 represents the Temkin adsorption isotherm using the obtained data from EIS technique as an example.

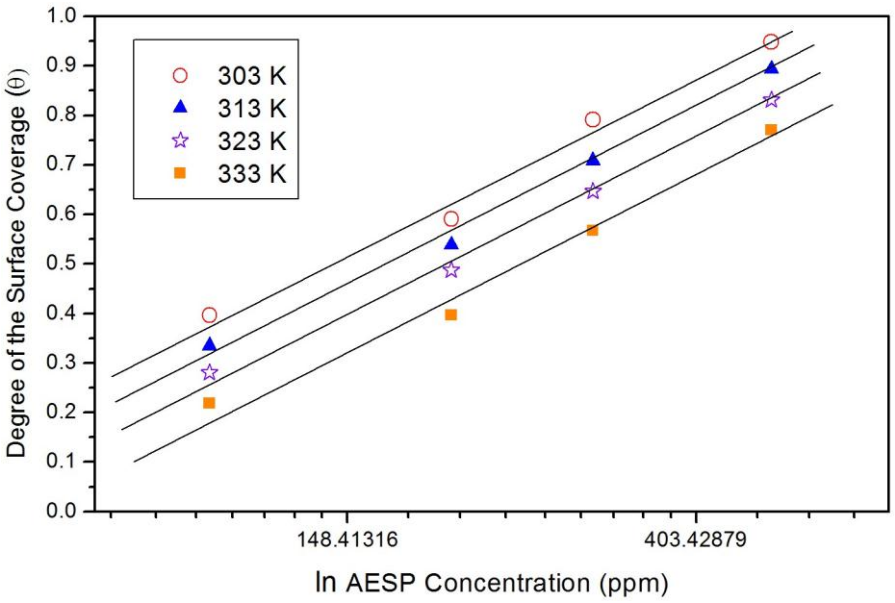

Figure 5. Temkin isotherm plots of LAS in 1 M HCl solution with various concentrations of AESP at different temperatures (data obtained from EIS technique).

From the intercepts and slopes of the straight lines of Temkin isotherm curves, values of equilibrium constant (K_{ads}) were calculated and given in Table 6. The analysis of the obtained data listed in Table 6 indicates that the values of K_{ads} decrease with increasing temperature. This confirms the suggestion that the strength of adsorption decreases with the increasing temperature and the inhibitor species are more readily removed from the steel surface [47-49].

Table 6. Equilibrium constant of adsorption for AESP at different temperatures associated with different techniques

Technique	Equilibrium constant of the adsorption (K_{ads})			
	303 K	313 K	323 K	333 K
Tafel	9482.4	6635.4	4995.9	3954.3
EIS	8547.9	7237.8	6061.5	4512.4
EFM	9926.3	7348.6	5499.1	4614.7

The equilibrium constant of adsorption, (K_{ads}) is related to the standard free energy of adsorption, (ΔG^{o}_{ads}) with the following equation [50-52]:

$$K_{ads} = \frac{1}{55.5} \exp\left(\frac{-\Delta G^{o}_{ads}}{RT}\right) \quad (6)$$

where R is the universal gas constant and T is the absolute temperature. The value of (55.5) is the concentration of water in the solution in mole/liter. The values of standard free energy of adsorption (ΔG^{o}_{ads}) obtained from different techniques are listed Table 7.

Table 7. Standard free energy of adsorption for AESP at different temperatures associated with different techniques

Technique	Standard free energy of adsorption (ΔG^{o}_{ads})			
	303 K	313 K	323 K	333 K
Tafel	-32.09	-32.19	-32.59	-32.96
EIS	-31.84	-32.51	-33.12	-33.39
EFM	-32.21	-32.55	-32.86	-33.44

The calculated values of standard free energy of adsorption (ΔG^{o}_{ads}) are negative and less than the threshold value of (-40 kJ mol^{-1}) required for chemical adsorption, indicating that adsorption of AESP on low-alloy steel surface in 1 M HCl is spontaneous and occurred according to the mechanism of physical adsorption [53-55].

3.7. Examination of surface morphology:

Formation of protective films of the inhibitor molecules on the electrode surface was further confirmed by scanning electron microscope (SEM).

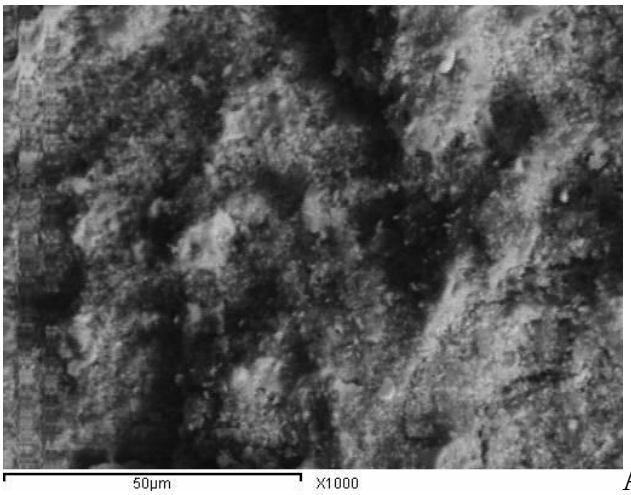

A

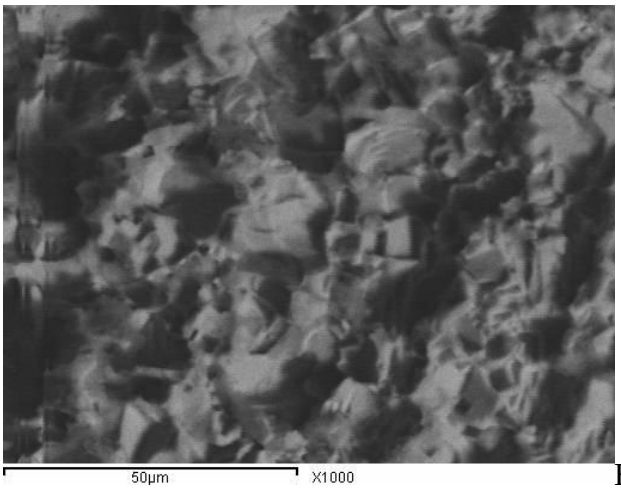

Figure 6. SEM photos of LAS samples after immersion for 24 hours in 1 M HCl solution in the absence (a) and presence of 500 ppm (b) of AESP at 303 K.

Figure 6 shows the SEM photos of LAS samples after immersion for 24 hours in static 1 M hydrochloric acid solutions, in the absence and presence of 500 ppm of AESP at 303 K. By the comparison of SEM images at the same magnifications, it is indicated that the corrosion of LAS coupons in the presence of AESP is weaker (Figure 6b) than in the case of absence of AESP (Figure 6a) that proves again the inhibiting effect of aqueous extract of Salvadora Persica against corrosion of low-alloy steel in 1 M HCl solutions.

3.8. Mechanism of inhibition

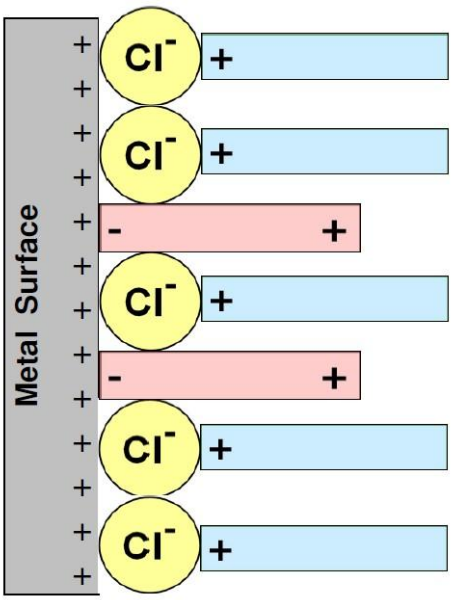

Figure 7. The proposed mechanism of inhibition of AESP in hydrochloric acid

The Salvadora Persica is composed by numerous naturally occurring organic compounds such as fatty acids (Oleic, linolic and stearic acids) [56], thiocyanate [23], alkaloids, Sulfur compounds as well as smaller amount of tannins and saponins [57]. These organic compounds contain aromatic rings, heteroatoms (sulphur, oxygen, nitrogen) and π electrons in their structure, which meet the general characteristics of typical corrosion inhibitors. Accordingly, the inhibitive action of AESP may be attributed to the adsorption of its components on the steel surface.

In aqueous acid solutions, these organic compounds of Salvadora Persica may exist either as neutral molecules or in the form of protonated molecules. It is known that the surface of steel samples acquires positive charges in aqueous acid solutions [58-60]. Moreover, some studies suggest that the chloride ions have a stronger tendency to adsorb on the metal surface [61,62].

Therefore, the adsorption of organic compounds of Salvadora Persica can occur via the already adsorbed chloride ions Cl^- on the positively charged steel surface. These adsorbed chloride anions Cl^- create an excess negative charge towards solution and favour more adsorption of organic cations leading to greater inhibition. Furthermore, the organic compounds of Salvadora Persica may be adsorbed on the positively charged steel surface in the form of neutral molecules, involving displacement of water molecules from the steel surface and sharing electrons with the steel surface [63]. Figure 7 illustrates the proposed mechanism for inhibition of AESP in HCl acid

4. CONCLUSION

The effectiveness of aqueous extract of Salvadora Persica as a novel green corrosion inhibitor for low-alloy steel in 1 M hydrochloric acid solutions has been investigated using chemical methods (mass loss and ICP-OES) and electrochemical techniques (potentiodynamic polarization, electrochemical impedance spectroscopy and electrochemical frequency modulation) at temperatures ranging from 303 to 333 K. The following results can be drawn from this study:

- AESP can serve as an effective inhibitor for the corrosion of low-alloy steel in HCl acid.
- The protection efficiency was found to increase with an increasing concentration of AESP and decrease with temperature.
- The adsorption of AESP on low-alloy steel surface has obeyed Temkin adsorption isotherm and the values of standard free energy of adsorption (ΔG^o_{ads}) reveal that AESP is adsorbed on low-alloy steel surface via physisorption mechanism.

ACKNOWLEDGEMENT

This work was financially supported by the Deanship of Scientific Research – JAZAN UNIVERSITY, Kingdom of Saudi Arabia under project number 2887/6/36. Authors are very grateful for this financial support.

References

1. G. Mann, “High Temperature High Pressure Electrochemistry in Aqueous Solutions”, NACE-4,

Houston, (1976) p34.
2. W. Ghanem, F. Bayyoumi, B. Ateya, *Corros. Sci.*, 38 (1996) 1171.
3. M. Majnouni and A. Jaffer, Chemical Cleaning of An Industrial Boiler –An Overview. International Water Conference paper no. IWC-03-34, 2003, 1.
4. McCoy JW, Industrial chemical cleaning, Chemical Publishing Co., ISBN 0-8206-0305-8, New York, 1984.
5. S. Sathiyanarayanan, C. Jeyaprabha, S. Muralidharan and G. Venkatachari, *Appl. Surf. Sci.*, 252 (2006) 8107.
6. H Ashassi-Sorkhabi and E Asghari, *Electrochim. Acta*, 54 (2008) 162.
7. N. Patel, S. Jauhariand, G. Mehta, S. Al-Deyab, I. Warad and B. Hammouti, *Int. J. Electrochem. Sci.*, 8 (2013) 2635.
8. D. Bouknana, B. Hammouti, H. caid, S. Jodeh, A. Bouyanzer, A. Aouniti, I. Warad, *Int. J. Ind. Chem.*, 6 (2015) 233.
9. D. Verma and F. Khan, *Green Chem. Lett. Rev.*, 9 (2016) 52.
10. M. Ameer and A. Fekry, *Turk. J. Chem.*, 39 (2015) 1078.
11. L. Nnanna, G. Nnanna, J. Nnakaife, N. Ekekwe, P. Eti, *Int. J. Mater.Chem.*, 6 (2016) 12.
12. M. Al-Otaibia, A. Al-Mayoufa, M. Khana, A. Mousaa, S. Al-Mazroab, H. Alkhathlan, *Arab. J. Chem.*, 7 (2014) 340.
13. D. Shuduan, and L. Xianghong, *Corros. Sci.*, 55 (2012) 407.
14. M. Al-Otaibi, M. Al-Harthy, A. Gustafsson, A. Johansson, R. Cleasson and B. Angmar-Mansson, *J. Clin. Periodontol.*, 31 (2004) 1048.
15. K. Almas, *J. Contemp. Dent. Prac.*, 3 (2002) 27.
16. H. Darmani, T. Nusayr and A. AL-Hiyasat, *Int. Dent. Hygiene*, 4 (2006) 62.
17. K. Almas, N. Skaug and I. Ahmad, *J. Dent. Hygiene*, 3 (2005) 18.
18. A. Mahar, and A. Malik, *Scient. Sindh J. Res.*, 8 (2001) 31.
19. N. Savithramma,Ch. Sulochana and K. Rao, *J. Ethnopharmacol.*, 113 (2007) 54.
20. S. Ezmirly, J. Cheng and S. Wilson, *Planta Medica*, 35 (1979) 191.
21. S. Abdel Waheb, M. Selim and N. EI-Fiki, *Bull Fac Pharm.*, 28 (1990) 67.
22. A. Bader and G. Flamini, *J. Essent. Oil Res.*, 14 (2002) 128.
23. A.Christy, L.Darout and N. Skaug, *Trends Appl. Spectrosc.*, 3 (2001) 25.
24. F. Howaida, S. Nils, M. Ann and W. George, *Pharma. Bio.*, 41 (2003) 399.
25. H. Abd El Rahman, N. Skaug, A. Whyatt and G. Francis, *Pharma. Bio.*, 41 (2003) 399.
26. H. Abdel-Fatah, A. Hassan, Z. Saadi, M. Shetify, H. El-Sehiety, *Chem. Sci. Trans.*, 3 (2014) 221.
27. H. Abdel-Fatah, Anti-Corros. Methods and Mater. 2012, 59, 23.
28. H. Abdel-Fatah, S. Rashwan, S. Abdel-Wahaab and A. Hassan, *Arab. J. Chem.*, 2011, ARTICLE IN PRESS.
29. H. Abdel-Fatah, H. Abdel-Samad, A. Hassan and H. El-Sehiety, *Res. Chem. Intermed.*, 40 (2014) 1675.
30. H. Abdel-Fatah, M. Kamel, A. Hassan, S. Rashwan, S. Abd El Wahaab and H. El-Sehiety, *Arab. J. Chem.*, 2013, ARTICLE IN PRESS.
31. R. Bosch, J. Hubrecht, W. Bogaerts and B. Syrett, *Corrosion*, 57 (2001) 60.
32. M. Fontana, "Corrosion Engineering," 3rd Edition, McGraw-Hill Book Company, New York, USA, 1987.
33. K. Alaneme, S. Olusegun and O. Adelowo, *Alex. Eng. J.*, 55 (2016) 673.
34. H. Gerengi, H. Goksu, P. Slepski, *Mat. Res.*, 17 (2014) 255.
35. M. El-Haddad and K. Elattar, *Int. J. Ind. Chem.*, 6 (2015) 105.
36. B. Mehdi, B. Mernari, M. Traisnel, F. Bentiss and M. Lagrenee, *Mater. Chem. Phys.*, 77 (2002) 489.
37. C. Cao, *Corros. Sci.*, 38 (1996) 2073.

38. M. Behpour, S. Ghoreishi, N. Mohammadi, N. Soltani and M. Salavati-Niasari, *Corros. Sci.*, 52 (2010) 4046.
39. M. Lebrini, M. Lagrenée, H. Vezin, M. Traisnel and F. Bentiss, *Corros. Sci.*, 49 (2007) 2254.
40. J. R. Macdonald and W.B. Johanson, John Wiley & Sons (1987) New York.
41. F. Mansfield, Corrosion Mechanism (1987) Marcel Dekker, New York.
42. E. McCafferty and N. Hackerman, *Electrochem. Soc*., 119 (1972) 146.
43. G. Avci, *Colloids Surf. A,* 317 (2008) 730.
44. S. Abd El-Maksoud and A. Fouda, *Mater. Chem. Phys.*, 93 (2005) 84.
45. E. Oguzie, C. Unaegbu, C. Ogukwe, B. Okolue and A. Onuchukwu, *Mater. Chem. Phys*., 84 (2004) 363.
46. D. Duong, Imperial College Press, (1980) London, UK.
47. S. Keera and M. Deyab, *Colloids and Surfaces A: Physicochem. Eng. Aspects,* 266 (2005) 129.
48. M. El Azhar, M. Traisnel, B. Mernari, L. Gengembre, F. Bentiss and M. Lagrenee, (2002) *Appl. Surf. Sci.*, 185 (2002) 197.
49. S. Abd El Rehim, H. Hassan, M. Amin, *Mater. Chem. Phys.*, 78 (2002) 337.
50. H. Ashassi-sorkhabi, B. Shaabani, B. Aligholipour and D. Seifzadeh, *Appl. Surf. Sci.,* 252 (2006) 4039.
51. E. Oguzie, *Pigment and Resin Technol.,* 34 (2005) 321.
52. S. Arab and A. Turkustuni, *Portugalia Electrochim. Acta*, 24 (2006) 53.
53. S. Bilgic and M. Sahin, *Mater. Chem. Phys*., 70 (2001) 290.
54. E. Ebenso, U. Ibok, U. Ekpe, S. Umoren, O. Abiola, N. Oforka and S. Martinez, *Trans. SAEST.*, 39 (2004) 117.
55. N. Eddy and A. Ekop, *J. Mater. Sci.*, 4 (2008) 10.
56. H. Abd El Rahman and N. Skaug, *Pharma. Bio.*, 41 (2003) 399.
57. M. Farooqi and J. Srivastava, *Quart. J. Crude Drug. Res.*, 8 (1968) 1297.
58. M. Yadav, L. Gope and T. Sarkar, *Res. Chem. Intermed.*, 42 (2016) 2641.
59. M. Lagrenee, B. Mernari, M. Bouanis, M. Traisnel and F. Bentiss, *Corros. Sci.*, 44 (2002) 573.
60. R. Solmaz, G. Kardas, B. Yazc, and M. Erbil, *Colloids Surf A Physicochem Eng Aspects*, 312 (2008) 7.
61. M. Quraishi and R. Sardar, *Mater. Chem. Phys.*, 78 (2002) 425.
62. X. Wang, Y. Wan, Q. Wang, F. Shi, Z. Fan, Y. Chen, *Int. J. Electrochem. Sci.*, 8 (2013) 2182.
63. R. Karthik, G. Vimaladevi, S. Chen, A. Elangovan, B. Jeyaprabha, P. Prakash, *Int. J. Electrochem. Sci.*, 10 (2015) 4666.